GEOMETRIC CONSIDERATIONS IN THE EXPERIMENTAL AND FINITE ELEMENT ANALYSES OF THE MICRODROPLET TEST

A. Hodzic, S. Kalyanasundaram, A. E. Lowe and Z. H. Stachurski

Department of Engineering, Faculty of Engineering and Information Technology
The Australian National University, ACT 0200, Canberra, Australia

SUMMARY: The microdroplet test has been used to establish the interfacial shear strength of the fibre-matrix bond in a specimen consisting of a fibre with a drop of cured resin. The fibre is pulled out while the drop is being supported by a platinum disc with a hole. This study has shown that geometry of the microdroplet test has the foremost influence on the stress distribution in the specimen and leads to two failure modes. Finite element analysis has been used for simulation of various features of the specimen's geometry. Stress distribution has been investigated along the specimen's interface and at the supported area of the droplet's surface. Results have shown the droplet's conus angle (at the droplet's tip) and the position of the fixture that is used to support the specimen during the test to be the two most influential parameters for the stress distribution in the specimen. By different combinations of these two parameters it is possible to influence the desired failure mode. Experimental results have firmly confirmed the FEA results leading to further understanding of the interfacial shear stress distribution of the fibre-droplet bond.

KEYWORDS: interface, interphase, silane coupling agent, microdroplet test

INTRODUCTION

The strength of the fibre - matrix bond in composite materials is essential in determining the bulk material properties. Chemical optimisation of the interfacial bond to give better properties of composite fracture toughness and strength has been in the focus of single fibre testing over last two decades. The microdroplet test has been designed to measure the interfacial shear strength of the fibre-matrix bond [1], but due to a complexity of the specimen's geometry, as shown in Fig. 1, the results contain a significant scatter in data. Before this test is used for a comparison of bonds in composite materials, it is important to quantify the ultimate shear stress that leads to debonding of the droplet from the fibre.

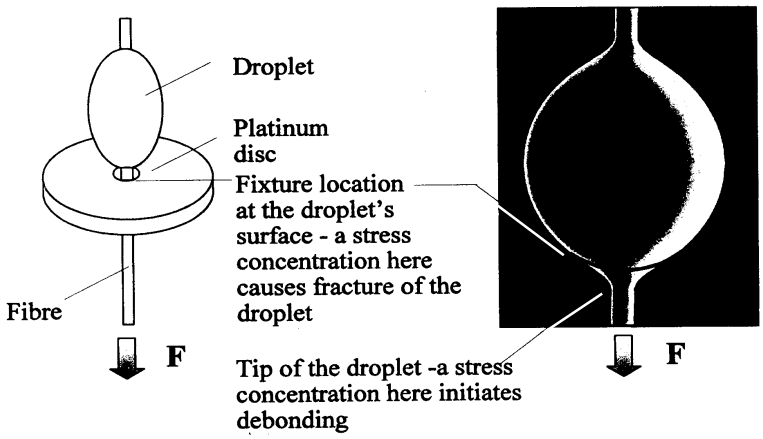

Fig. 1. Schematic view of the microdroplet test and SEM image of the untested specimen showing the regions where higher stresses occur during the test.

The common approach is that the average shear stress τ_{av}, with a constant stress distribution, is assumed along the interface between the fibre and the droplet:

$$\tau_{av} = F/(d\pi l) \quad (1)$$

where F is the applied load, d is the fibre's diameter and l is the embedded length of the specimen.

In our previous work [2, 3] it was noticed by means of finite element analysis that the specimen's interface had non-uniform stress distribution. A high stress concentration at the tip of the droplet was assumed to be responsible for the initiation of the debonding failure mode. The supported area at the droplet's surface also suffered high stress concentration that caused a breakage of the droplet and partial debonding of the upper part of the droplet. These two failure modes were recorded in 98% of results. Each of these failure modes is associated with a different failure mechanism. The full debonding of the droplet from the fibre is assumed to be initiated by the stress concentration at the tip of the droplet, while the partial debonding of the droplet from the fibre is caused by crack propagation from the supported area at the surface of the droplet. The full debonding failure mode provides the information on the interfacial shear strength. Therefore, this investigation has been focused on the understanding of both failure modes in order to predict the desired result - the fully debonded specimen. Also, it was found important to include the influence of different parameters of the test and specimen's geometry to the stress analysis of the microdroplet test data.

It has been shown by work of other authors, that geometry of the specimen and the testing rig [4, 5] had a strong influence on the results of the experiment. The theoretical model of the microdroplet specimen has evolved from a cylinder [6] to an ellipsoid [7] which included elliptic geometry to the stress analysis. However, as the bottom of the ellipsoid ends on the fibre, the conus angle is 90 degrees, therefore the influence of this parameter was not considered in this model.

Very important measurements of the stress distribution have been carried out by means of Raman spectroscopy [8-11] where it was noticed that the stress distribution at the interface was far from linear and was dependant on a surface treatment of the fibres.

In conclusion, it seems important to describe the major geometric effects in the stress distribution of the interface in the microdroplet specimen, and to obtain the stress equation that includes influential parameters. Since the wider scope of this study is to determine the effect of environmental attack in marine based composites on the interfacial region, use of the microdroplet test is advantageous due to the small amount of material required, and the absence of complex stress transfer mechanisms present in bulk composites. However, the scatter in the microdroplet test data needs to be significantly reduced in order to enable this experimental technique to be used in the investigation of water aging of composite materials interfaces.

1. FINITE ELEMENT ANALYSIS

Finite element analysis of the microdroplet test was carried out using STRAND6 software and the model was treated as a linear axisymmetric problem. The model comprised approximately 8-10 000 plate elements and the interphase region was modelled as seven layers of functional change in material properties such as elastic modulus and Poisson's ratio. The mesh is shown in Fig. 2(a). Fig. 2(b) shows an enlarged image of the epoxy droplet and glass fibre, where the central part of the droplet is in a shape of a ball and two sides in a shape of a conus each with a small radius ending on the fibre. 2D section of a ball with a conus at each end has been the basic model for the droplet in the FEA. Also, the bonding radius (the radius between the droplet's conus and the fibre) has been included in the FEA model in order to make it close to the shape of the real specimen. Two major parts of the modelling included variation of parameters of geometry and material properties of the interphase.

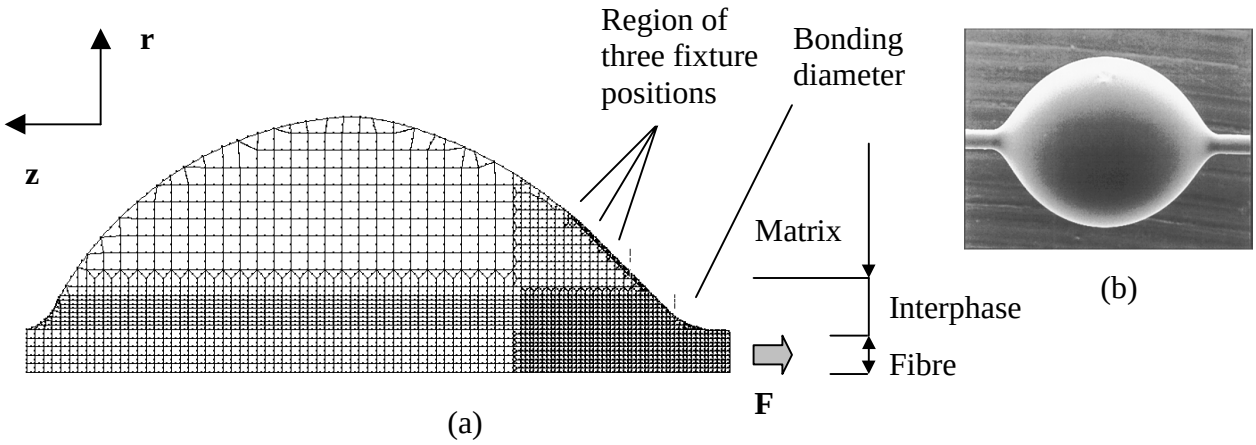

Fig. 2. (a) 2D mesh of the microdroplet specimen used in FEA and (b) SEM image of the epoxy droplet and glass fibre portraying the specimen's shape used for the mesh.

1.1 Variation Of The Specimen's Geometry

1.1.1 Droplet

A preparation for the FEA modelling of the microdroplet included recording scanning microscope images of specimens and measurements of the actual epoxy/glass specimens' geometry. It was concluded that the droplet's length, diameter and conus angle were correlated by a linear increase and the functions were established. The observed correlations were applied in the FEA model of the droplet. Influences of the droplet's length (i.e. embedded length of the specimen) and diameter on the shape of the specimen's stress distribution were investigated and were found negligible since the high stresses were located at the bottom of the droplet and were not influenced by a change in the specimen's size. Two parameters of the droplet's geometry were varied: the conus angle and the bonding diameter. Droplet's length and diameter followed the change of the conus angle in order to maintain the original shape of the droplet. Variation in the conus angle included three values of this parameter: 80^o, 90^o and 100^o, while the bonding diameter remained a constant value. Variation in the bonding diameter also included three values: 25^o, 30^o and 35^o while the conus angle remained constant.

1.1.2 Fixture

Variation of the supporting hole size was modelled as a change in position of the fixed boundary conditions along the droplet's surface. Three fixed nodes representing the hole's edge were moved relatively closer to the fibre as diameter of the hole was decreased. Values for the hole's sizes were taken according to the available sizes of the disc apertures that were later used in the experimental part of this work: 30, 40 and 50 μm hole diameters, for a given load of 160 mN.

1.2 Variation Of The Interphase Properties

Interphase is a chemically affected region around the fibre in the fibre-matrix bond, due to the presence of the silane coupling agent. The interphase was modelled as seven adjacent layers with functional changes in material properties, starting from the fibre in radial direction. Eight different functions were varied through the interphase properties as shown in Table 1. The layers were modelled as plates having dimensions of 1 μm each in radial direction, forming the layers along the full length of the specimen in the axial direction, as shown in Fig. 2(a).

1.3 Results Of The FEA

1.3.1 Droplet

The Von Mises stresses of two important regions in the microdroplet specimen's FEA model were analysed: along the droplet's surface where the high stresses were initiated by the fixed boundary conditions at the fixture's position, and along the interface, defined as the boundary line between the fibre and the first layer of the interphase.
Variation of the bonding diameter showed an insignificant change in the stress distribution of the interface or the droplet's surface. The influence of this parameter was not taken into consideration.
Variation of the conus angle was discussed in detail in our previous work [2]. In this work the same variation has been performed using glass/epoxy material properties, in order to compare the influences of the conus angle and the fixture position to the stress distribution in the epoxy/glass specimen.

1.3.2 Fixture

The influence of the fixture position (size) on the trend of the stress distribution along the interface was found notable in the case of 30 μm hole diameter, as shown in Fig. 3. However, the stresses at the droplet's tip (z=6μm), assumed to be responsible for the initiation of the debonding failure mode, were not significantly affected by this variation. In our previous work [2] it was shown that the change in the position of the fixture due to the variation in the conus angle could not significantly influence the stress at the interface region. In that case, the stress peak at the droplet's tip was influenced only by the variation in the conus angle.

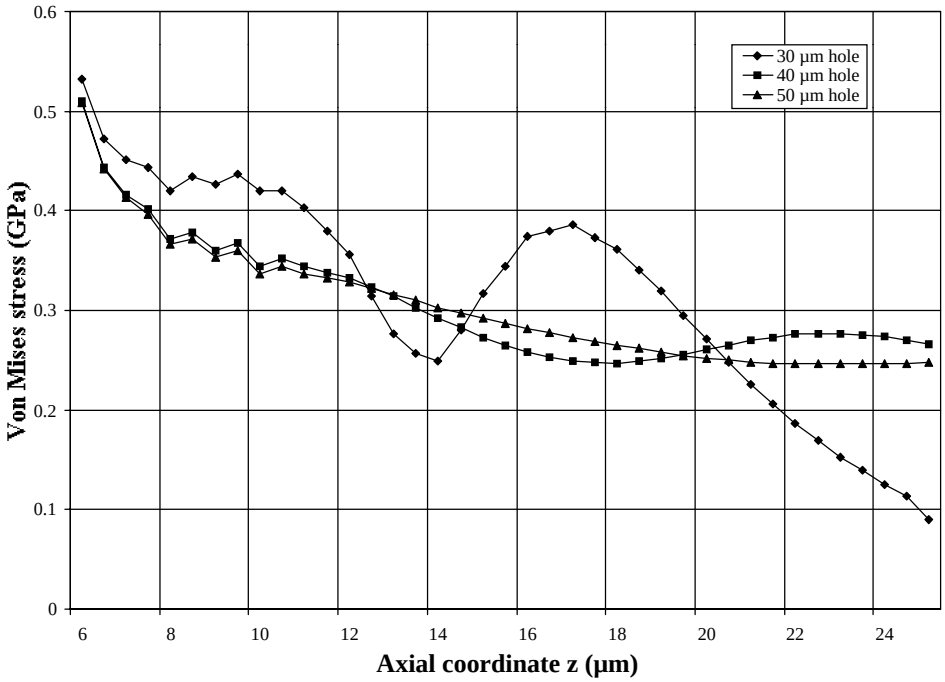

Fig. 3. Distribution of von Mises stress along the interface for different disc hole diameters.

The stresses at the droplet's surface were found strongly affected by the change in fixture size, as shown in Fig. 4. As the fixture was closer to the droplet's tip (smaller size hole), the stress peak at the fixture region was significantly higher. The stress peaks were taken at the same distance (1 μm) from the fixed region in each case.
The stress increase indicated that the failure mode could be influenced by the position of the fixture, i.e. the diameter of the disc hole. Increasing the hole size it is possible to influence the stress peak at the droplet's surface to be less than the stress peak at the interface. This could improve consistency in the microdroplet test results causing more specimens to be fully debonded.

1.3.3 Variation of the interphase properties

The interphase properties were varied whilst the geometric conditions and the applied load of 160 mN were kept constant. The eight functions that were used for the simulation of different properties of the interphase region could be separated in two groups as shown in Table 1: the strong and the weak interphase region. The strong interphase region included stronger material properties than the epoxy resin and vice versa.

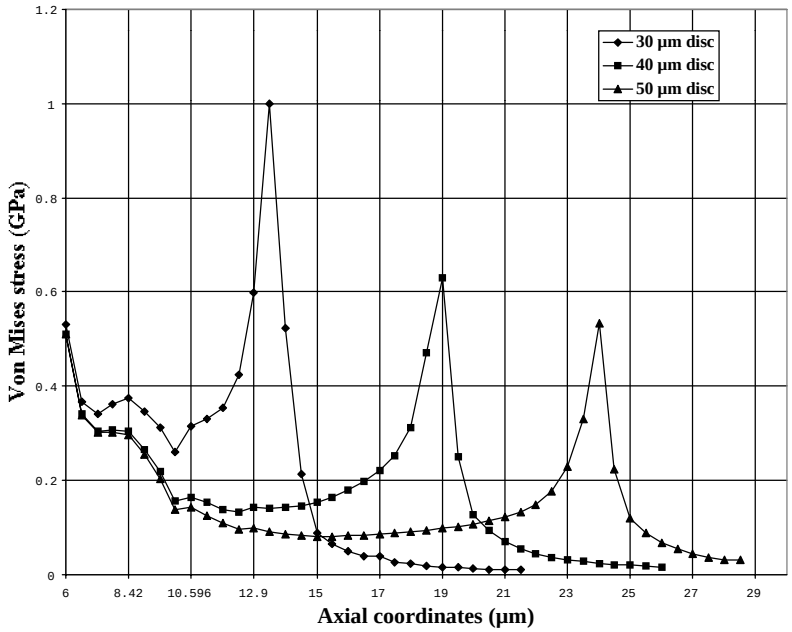

Fig. 4. Distribution of von Mises stress along the droplet's surface for different disc hole diameters.

Table 1. Functional variations of the interphase properties

Legend	Function	Description	Group
int = mat	E,ν = const	Interphase props.= matrix props.	weak
lindec	E,ν = A-B(x)	Linear decay of props. of interphase	strong
step	E,ν = const	Interphase props.= const. middle value > matrix	strong
pit	E,ν = const	Interphase props.= const. < matrix props.	weak
expup	E,ν = $A+Be^{x}$	Exponential increase in props. of interphase	weak
hill	E,ν = $A+Be^{1/x}$	Exponential increase in props. of interphase	weak
fall	E,ν = $A-Be^{x}$	Exponential decay in props. of interphase	strong

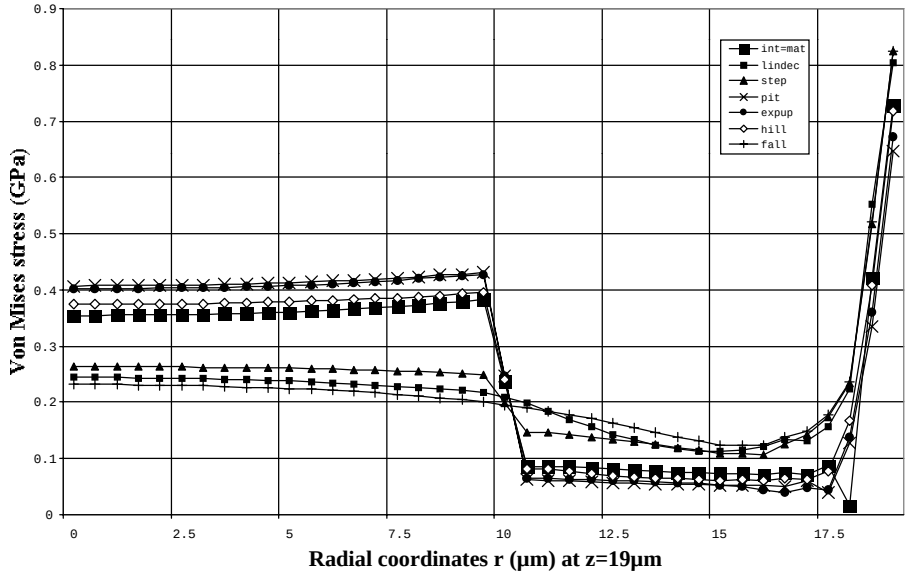

Fig. 5. Distribution of von Mises stress along the fibre-interphase-matrix section at z = 19 μm for different functional variations of the interphase.

The stresses in radial direction at z = 19 μm across the fibre-interphase-matrix region (1 μm distance below the fixture region) are shown in Fig. 5. The results showed that the stresses were visibly grouped in two trends, the strong and the weak interphase behaviour. The trends of the strong interphase region group had approximately constant transition from the fibre through the interphase, and the sudden increase at the droplet's surface. The trends of the weak interphase region group had significantly higher stresses in the fibre, sudden drop at the first layer of the interphase and lower stresses in the droplet than the strong interphase group. The stress peaks at the droplet's surface were also lower than that of the strong interphase group.

The analysis of the stress distribution along the interface region showed significantly different behaviour between the weak and the strong interphase group, as shown in Fig. 6. At the droplet's tip, the stresses of the weak interphase group had approximately the same value while the stresses of the strong interphase group significantly differed. As the material properties of the interphase were stronger, the stress at the droplet's tip had a higher value.
These results indicated that the quality of the interphase region has a strong influence on the stress distribution in the microdroplet test. The material properties of the interphase region need to be established in order to obtain the accurate stress value at the droplet's tip region. Qualitatively different interphase properties resulted in various stress distributions for the given applied load. The stresses at the droplet's tip of the weak interphase regions exhibited consistent results, while the functional decay in material properties of the strong interphase group had a major role in the stress values of that region. This phenomenon indicated that the change in material properties of the interphase should be established prior to testing of the microdroplet specimen.

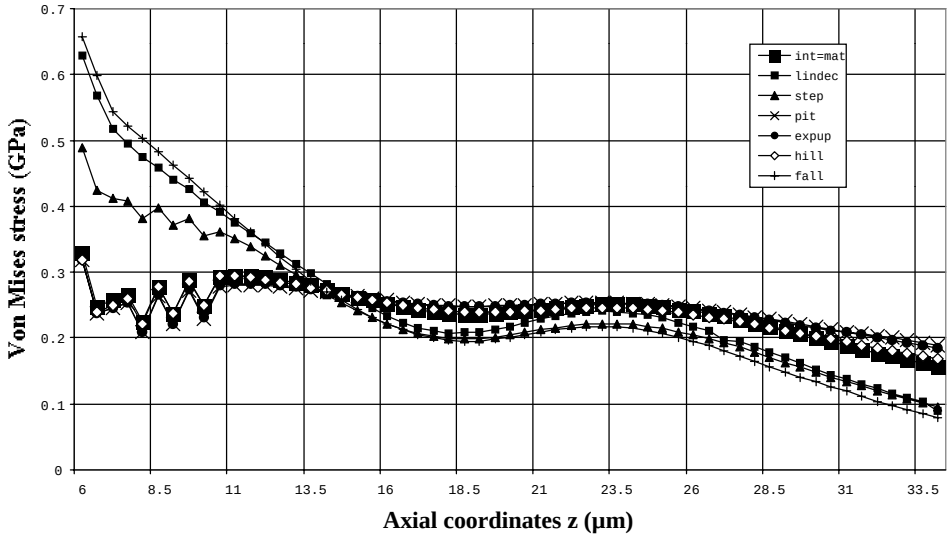

Fig. 6. Distribution of von Mises stress along the interface for different functional variations of the interphase.

2. EXPERIMENTAL WORK

Experimental work was carried out using E-type glass fibres, 20 μm in diameter, taken from a unidirectional tape of 450 g/m^2 density. Epoxy resin Ciba-Geigy Araldite F/GY260 was mixed with Piperidine in the ratio 35g: 2cc. Two sets of the microdroplet specimens were produced in various sizes and cured in an oven for 16 hours at 120^{o}C. The testing procedure is explained in details in our previous work [2]. All tests were performed using an Instron

model 4505 Universal Test Frame, with a 10N load-cell and a special jig to hold the platinum disc.
Images of the specimens before testing were obtained using an optical microscope connected to a digital video camera in order to record specimen's geometry, and by fractographic analysis after the test, in order to determine a failure mode and possible deformation of the each specimen.
Platinum disc apertures of 30, 40 (45) and 50 μm hole size were used to support the specimens during the test, in order to investigate the influence of the hole size on the resulting force in the microdroplet test.

2.1 Experimental Results

The first set of specimens was fully cured as determined by the fractographic analysis, while the other set was slightly undercured due to an incoherent mixture of the resin and catalyst. A deformation of the droplets of the undercured set of specimens was above the elastic limit. However, the results of both sets of specimens are presented here since similar behaviour was detected and some common conclusions derived.

2.1.1 Force-displacement diagrams

The specimens of the fully cured set of droplets had a consistent force-displacement behaviour, as shown in Fig. 7(a). The trend of all specimens was a perfectly linear increase with the sudden drop after the droplet's failure. This trend was independent on the failure mode; it exhibited the same linear correlation both for partially and fully debonded specimens. For the same size of the specimen, partial failure mode produced a lower maximum peak than the fully debonded specimen. This indicated that the partial failure follows the same trend as the full debonding failure but the crack at the droplet's surface brakes the specimen in two before its maximum interfacial shear strength is reached. In both cases the force-displacement diagram exhibited resistance of the interface to the force, but the partial failure mode did not provide the full information on the interfacial shear strength.
The specimens of the undercured set showed a different trend in the force-displacement diagram as shown in Fig. 7(b). The correlation was not perfectly linear and the peak was curved for both failure modes. This indicated that the specimens were not fully cured, and the same conclusion was obtained as for the specimens of the first set, that the trend of F-d curve was similar for the full and partial failure modes.

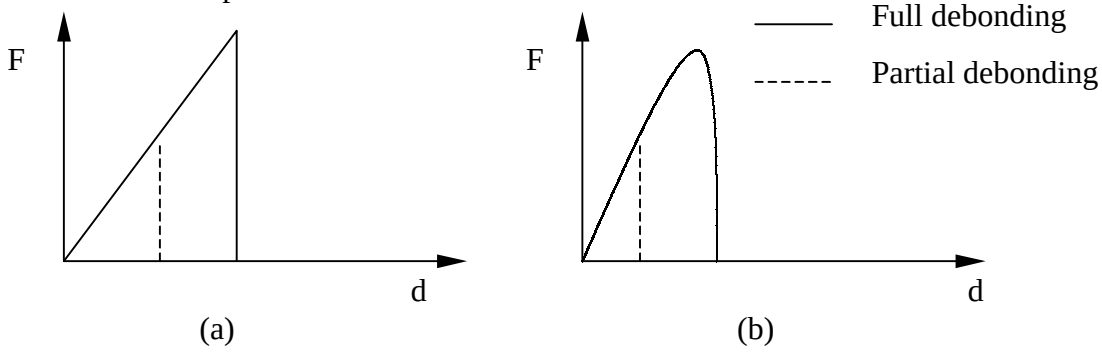

Fig. 7. Force-displacement diagrams for (a) cured specimens and (b) slightly undercured specimens.

2.1.2 The influence of the hole size to the test results

Variation of the hole size resulted in a major difference in the trends of each hole size group of specimens. Basically, the experimental results confirmed the findings of the previous FEA, where the change in size of the fixture strongly affected the stress distribution in the specimen and consequently the failure mode. The images of different failure modes are presented in Fig. 8 (a, b, c). The fully debonded specimen, tested with the 50 μm aperture, failed at the droplet's tip before the plastic deformation at the droplet's surface broke the specimen in two,

as shown in Fig. 8(a). The broken specimen was tested with the 30 μm aperture and the stress concentration at the droplet's surface was stronger than that at the droplet's tip, as shown in Fig. 8(b). The specimen that failed by the mixed mode, at the droplet's tip and the droplet's surface at the same instant, was tested with the 45 μm aperture, as shown in Fig. 8(c). These three specimens are the representatives of the hole size influence to the failure mode, although the each hole size group contained different failure modes.

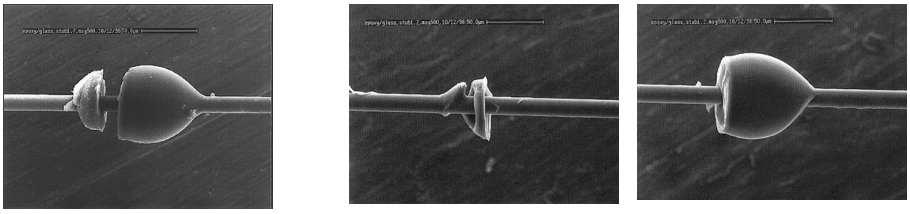

(a) (b) (c)

Fig. 8. Different failure modes in the microdroplet test: (a) fully debonded droplet, (b) partially debonded (broken) droplet and (c)mixed mode of the previous two modes.

The force/droplet's size ratio was different for the each hole size group of specimens, as shown in Fig. 9 (a, b), for both sets of specimens. As the hole size was larger, the average force/diameter ratio was higher for the fully cured and undercured specimens. For the same size of specimens, the debonding force was higher if a bigger hole size was used. This confirmed the FEA results that showed that the stress concentration at the fixture region was lower for the larger hole size, therefore the crack was not initiated at the droplet's surface and more time was available for the full debonding process.
The droplet's diameter is here taken as the representative parameter of geometry since it was the most convenient measurement from the droplet's image; however, the droplet's length and conus angle are linearly correlated to the diameter of the epoxy droplets, therefore any of these parameters could be used instead. It was noticed that the linear correlation between the force and the conus angle had the strongest increase hence it could be concluded that the conus angle had the most influential role among the parameters of the droplet's geometry.

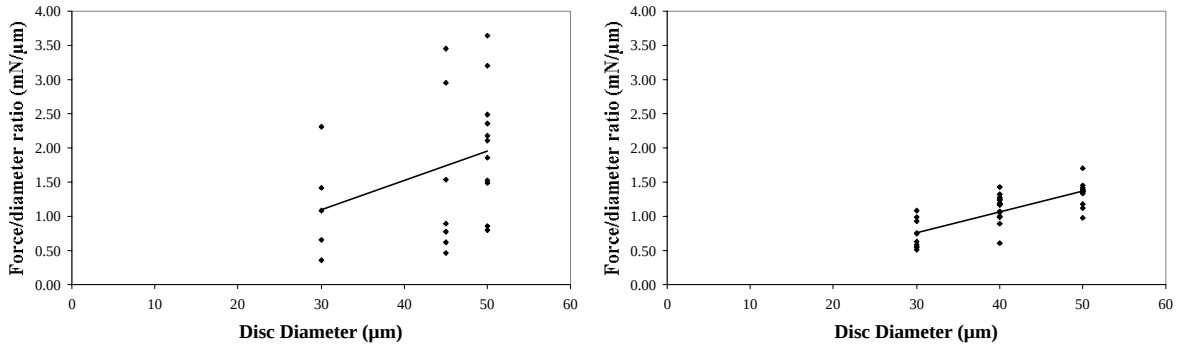

(a) (b)

Fig. 9. Force/displacement ratio vs disc hole size for (a) fully cured and (b) slightly undercured specimens.

The force/diameter ratio in correlation with the diameter is shown in Fig. 10(a,b). Three different linear trends are associated with three different hole sizes. The results have shown that the fully debonded specimens were of larger diameters (conus angles) and tested with 45 and 50 μm hole size. The results of 50 μm hole size had the highest percentage of fully debonded specimens, as predicted by FEA.
Specimens of all sizes tested with the 30 μm hole size resulted in only partial debonding. Specimens of smaller diameters (conus angles) tested with any hole size also resulted in partial debonding. This confirmed the predictions of FEA, that both the conus angle and the fixture's hole size have dominant influence on the failure mode. The combination of the

certain size of the droplet and the certain fixture's hole size produced the fully debonded specimens, provided the information on the ultimate interfacial shear strength and proved that the partial failure mode could not be included as the valid result in the microdroplet test. It is fair to assume that the scatter in data, presented in many previous results of this experimental technique, has been the consequence of different failure modes included in the analysis of the experiment.

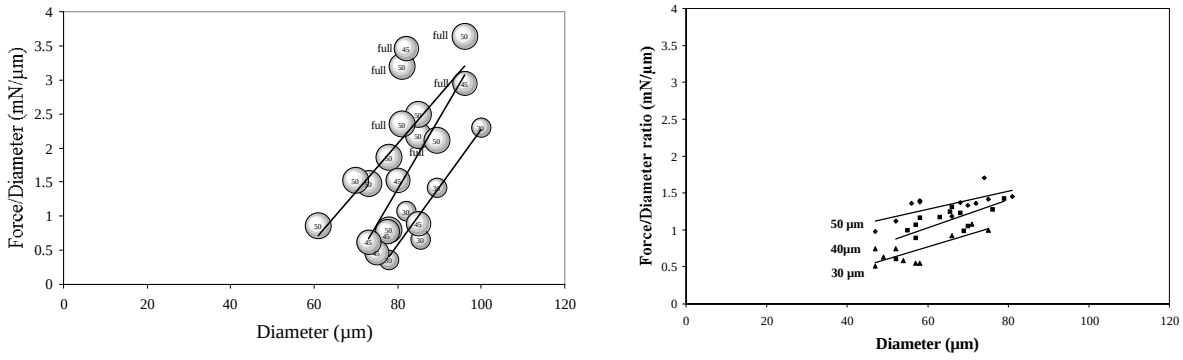

(a) (b)

Fig. 10. Force/diameter ratio vs diameter for (a) fully cured and (b) slightly undercured specimens.

DISCUSSION AND CONCLUSIONS

This work has shown that the droplet's conus angle and the fixture's hole size have tremendous influence on the test results in the microdroplet test. FEA has revealed that the stress concentration at the droplet's surface, due to the presence of fixture, was strongly affected by the position of the fixture i. e. the hole size. In our previous work it was shown by means of FEA that the conus angle had a significant influence on the stress concentration at the droplet's surface. Also, the variation of different material properties through the interphase, modeled as seven adjacent layers, has shown that the quality of this region has a significant influence to the stress distribution of the interface and needs to be investigated prior to testing.

The experimental work with epoxy/glass microdroplet specimens substantially confirmed the FEA results. The experimental results have shown that it was possible to reduce the stress concentration at the fixture region for epoxy/glass system by using a bigger hole size (45 and 50 μm) and selected size of specimens with larger conus angles (100º and more). The combination of these parameters led to the full debonding failure initiated at the droplet's tip instead from the droplet's surface. The desired results of this experimental technique are the fully debonded specimens since only that failure mode provides the information on the specimen's ultimate shear strength.

Specimens of smaller size (conus angle) failed at the surface by using all three hole sizes due to the stress concentration at the droplet's surface from the small conus angle. Specimens of all sizes tested with the 30 μm hole size also failed at the surface from the stress concentration caused by the position of the fixture, as predicted by FEA. In both cases the partial failure mode happened because the stress at the surface was higher than the stress at the droplet's tip causing the crack propagation from the droplet's surface to "interrupt" the process of debonding.

A simple mechanical analysis of the microdroplet test could give some answers to the specimen's behavior that was explained in this work. Fig. 11. shows a schematic view of the free body diagram in the microdroplet test. R and R' are the reaction forces of the fixture for the conus angles α and β respectively, their components Rn, Rt and Rn', Rt' are the associated normal and tangential projections respectively. The reaction R' of the conus angle β is placed further from the fibre, simulating a larger hole size.

In the case of the smaller conus angle and hole size, the tangential projection Rt is stronger causing the local tensile stress concentration. The normal projection Rn is weaker and due to the hole size the distance from the droplet's tip is shorter, therefore the moment about the

droplet's tip from this component is weak. This moment is assumed to be responsible for the stress concentration at the droplet's tip.
In the case of the larger contact angle (β) and hole size, the tangential projection Rt' is much weaker and consequently the local stress concentration is decreased. The normal component of reaction (Rn') is stronger; due to the larger hole size the distance from the droplet's tip is increased, and both of these factors cause the stronger moment about the droplet's tip therefore the higher stress concentration.

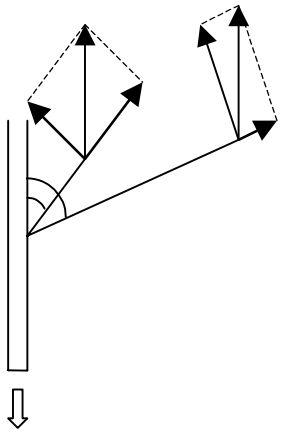

Fig. 11. 2D free body diagram of the lower part of the specimen where the load is applied and the droplet supported.

This has shown that the microdroplet test data could not be analyzed without quantifying the contributions from the conus angle and the fixture's placement to the stress distribution. It is necessary to determine the stress equation that will give a precise result of the shear stress value at the droplet's tip including the important parameters of the specimen and test geometry.

FUTURE WORK

The future work on the microdroplet test will include a theoretical analysis of the stress distribution along the interface of the specimen and the contribution of the previously discussed parameters of geometry to the stress value at the tip of the droplet. Once the stress analysis tool is established, the microdroplet test will be used for the investigation of the interfacial quality in water aged composite materials.

REFERENCES

1. B. Miller, P. Muri and L. Rebenfeld, "A Microbond Method for Determination of the Shear Strength of a Fiber/Resin Interface", *Composite Science and Technology* , 28, 1987, pp. 17-32
2. A. Hodzic, S. Kalyanasundaram, A. Lowe and Z. H. Stachurski, "The Microdroplet Test: Experimental and Finite Element Analysis of the Dependence of Failure Mode on Droplet Shape", *Composite Interfaces*, in press, 1999
3. A. Hodzic, S. Kalyanasundaram, A. E. Lowe and Z. H. Stachurski, "FEA Simulation and Stress Analysis of the Effect of Geometry on the Microdroplet Test", The Second Australasian Congress On Applied Mechanics, 10-12 February 1999, Canberra, *conference proceedings,* in press
4. C. T. Chou, U. Gaur and B. Miller, " The Effect of Microvise Gap Width on Microbond Pull-Out Test Results", *Composite Science and Technology*, 51, 1994, pp. 111-116

5. L. P. Hann and D. E. Hirt, "Simulating the Microbond Technique with Microdroplets", *Composite Science and Technology*, 54, 1995, pp. 423-430
6. R. J. Scheer and J. A. Nairn, "A Comparison of Several Fracture Mechanics Methods for Measuring Interfacial Toughness with Microbond Tests", *J. Adhesion*, 53, 1995, pp. 45-68
7. T. Schuller, U. Bahr, W. Beckeret, B. Lauke, "Fracture Mechanics Analysis of the Microbond-Test", *Composites Part A : Special Issue IPCM 1997*
8. C. Galiotis, "A Study of Mechanisms of Stress Transfer in Continuous- And Discontinuous-Fibre Model Composites by Laser Raman Spectroscopy", *Composites Science and Technology*, 48, 1993, pp. 15-28
9. R. J. Young, "Evaluation of Composite Interfaces Using Raman Spectroscopy", *Key Engineering Materials* , Vols. 116-117, 1996, pp. 173-192
10. R. J. Day and J. V. Cauich Rodrigez, "Investigation of the Micromechanics of the Microbond Test", *Composites Science and Technology*, in press
11. R. J. Young, Y.-L. Huang, X. Gu and R. J. Day, "Analysis of Composite Test Methods Using Raman Spectroscopy", *Plastics, Rubber and Composites Processing and Applications*, 23, 1995, pp. 11-19
12. Lawrence T. Drzal and Pedro J. Herrera-Franco, "Composite Fiber Matrix Bond Tests", *Reprinted from Engineered Materials Handbook*, Volume 3: Adhesives and Sealants, 1991, pp. 391-405
13. H. D. Wagner, "The Significance of Microcomposites as Experimental Models", *Polymer Composites*, 1991, Vol. 12, No. 4, pp. 233-236
14. W. Beckert and B. Lauke, "Critical Discussion of the Single-Fibre Pull-Out Test: Does It Measure Adhesion?", *Composites Science and Technology*, 57, 1997, pp. 1689-1706
15. E. Mader, "Study of Fibre Surface Treatments for Control of Interphase Properties in Composites", *Composites Science and Technology*, 57, 1997, pp. 1077-1088